Electronic Supplementary Information (ESI)

Synergistically Improved PIM-1 Membrane Gas Separation Performance by PAF-1 Incorporation and UV Irradiation

Rujing Hou[1], Stefan J. D. Smith[1], Kristina Konstas[2], Cara M. Doherty[2], Christopher D. Easton[2], Jaesung Park[3], Heewook Yoon[3], Huanting Wang[1], Benny D. Freeman[1,3*], Matthew R. Hill[1, 2*]

1: Monash Centre for Membrane Innovation, Department of Chemical and Biological Engineering, Monash University, Clayton, VIC 3169, Australia.

2: CSIRO, Manufacturing, Private Bag 10, Clayton South, VIC 3169, Australia

3: John J. McKetta Jr. Department of Chemical Engineering, The University of Texas at Austin, 2501 Speedway, Austin, TX, 78712, USA

* Corresponding authors: Matthew.Hill@csiro.au, matthew.hill@monash.edu;

freeman@che.utexas.edu, Benny.Freeman@monash.edu

1. Gel Permeation Chromatography

We used a Waters Alliance e2695 liquid chromatograph equipped with a Waters 2414 differential refractometer and 3× mixed C and 1 mixed E PL gel columns (each 300 mm × 7.5 mm) to obtain Gel Permeation Chromatography (GPC) for PIM-1 and UV irradiated PIM-1 from our laboratories. The eluent was tetrahydrofuran (THF) at 30 °C (flow rate: 1 mL min^{-1}). Number (*M*n) and weight-average (*M*w) molar masses were evaluated using Waters Empower Pro software. The GPC columns were calibrated with low dispersity polystyrene (PSt) standards (Polymer Laboratories), and molar masses are reported as PSt equivalents. A third order polynomial was used to fit the log *M*p vs time calibration curve, which was linear across the molar mass range 2×10^2 to 2×10^6 g mol^{-1}.

Table S1 **Gel Permeation Chromatography of PIM-1**

	M_n	M_w	M_p	M_z	M_{z+1}	Polydispersity
PIM	65938	241991	82881	1603418	3569787	3.7
PIM-0.5 h	15595	146206	71639	1450012	3647113	9.4
PIM-1.5 h	14695	144291	72379	1396922	3369165	9.8
PIM-3.0 h	15086	138977	70858	1391563	3576627	9.2
PIM-4.5 h	15408	137838	70906	1493342	3990324	8.9

Units: average molecular weight (M_w); number average molecular weight (M_n); molecular weight polystyrene equivalents weight (M_p); size average molecular weight (M_z); polydispersity=(M_w/M_n).

Notice: PIM: PIM-1 without UV irradiation, PIM-0.5 h, PIM-1.5 h, PIM-3.0 h, and PIM-1-4.5 h: PIM-1 with UV irradiation for 0.5h, 1.5 h, 3.0 h, and 4.5 h.

2. Isotherm Adsorption Curves

BET surface areas were calculated from nitrogen isotherms at 77 K. The BET surface area for PAF-1 is 3435 m^2/g.

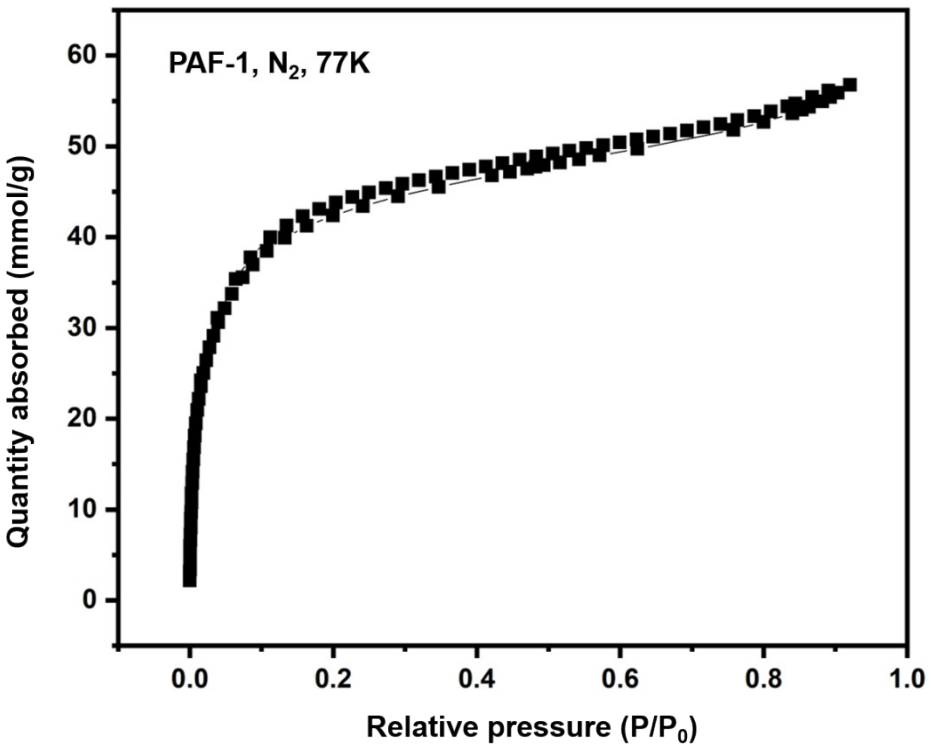

Figure S1: N_2 adsorption isotherm for the prepared PAF-1

3. Thermal Gravimetric Analysis (TGA)

Thermalgravimetric analysis of membranes was carried out using a Mettler Toledo TGA 2 STAR^e System thermogravimetric analyser from 50 °C to 800 °C at 10 °C/min under 50 ml/min nitrogen.

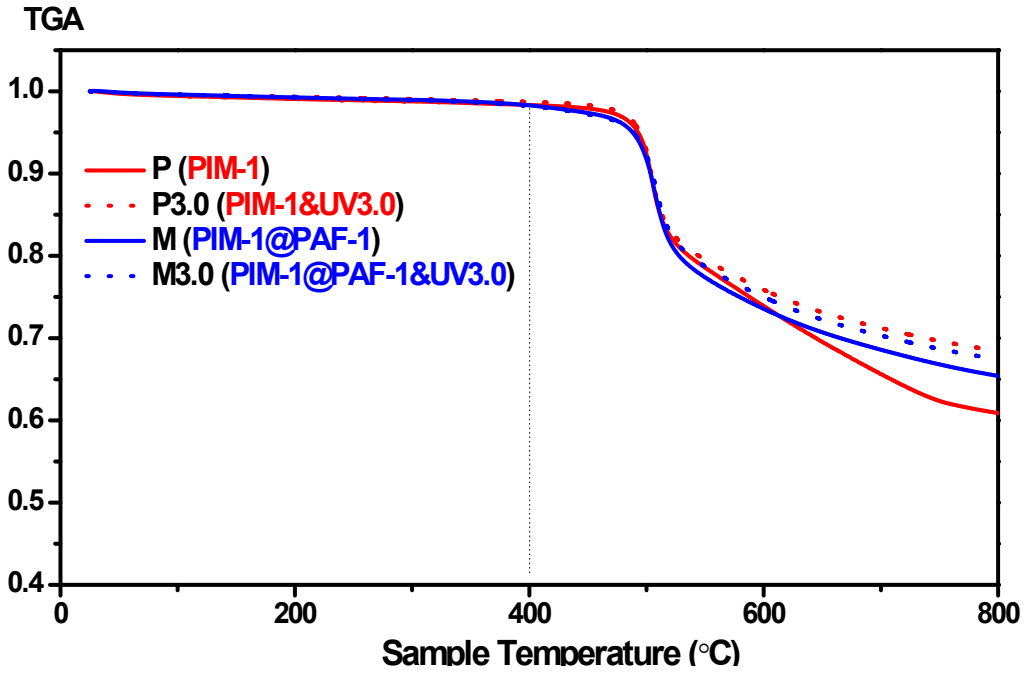

Figure S2. TGA results for samples P (PIM-1), P3.0 (PIM-1&UV3.0), M (PIM-1@PAF-1) and M3.0 (PIM-1@PAFF-1&UV3.0)

4. Membrane gas performance before and after UV irradiation -Single Gas

Pure gas permeabilities for H_2, N_2, CH_4, and CO_2 were calculated by using the constant volume and variable pressure method. The gas permeability is determined from the rate of permeate pressure increase (*dp/dt*) once permeation reaches a steady state, according to equation 1.

$$P = \frac{\frac{273 \times 10^{10}}{760} \frac{VL}{AT\left[\frac{P_2 \times 76}{14.7}\right]}\left(\frac{dp}{dt}\right)}{}$$ Equation 1

Where: P refers to the permeability of a membrane to a gas and its unit is in Barrer (1 Barrer = 1×10^{-10} cm^3 (STP)·cm/cm^2·sec·cmHg); V is the volume of the permeate chamber (cm^3), L is the film thickness (cm). A is the effective membrane area (cm^2); T is the temperature (K), and P_2 is the feed gas pressure (psia).

Ideal selectivity ($\alpha_{A/B}$) is stated as the ratio of single gas permeability for a given gas pair.

Table S2	Relative Permeability			
	P(H_2)	**P(N_2)**	**P(CH_4)**	**P(CO_2)**
P	1.00	1.00	1.00	1.00
P0.5	0.70	0.42	0.33	0.52
P1.5	0.66	0.17	0.10	0.27
P3.0	0.38	0.05	0.03	0.08
P4.5	0.19	0.01	0.01	0.01
M	1.00	1.00	1.00	1.00
M0.5	1.03	0.51	0.38	0.66
M1.5	0.66	0.15	0.09	0.21
M3.0	0.67	0.11	0.06	0.17
M4.5	0.22	0.03	0.02	0.03

5. Membrane Performance for Trade-Off Comparison

Table S3	Permeability (Barrer)				Ideal Selectivity				
	$P(H_2)$	$P(N_2)$	$P(CH_4)$	$P(CO_2)$	H_2/N_2	H_2/CH_4	H_2/CO_2	CO_2/CH_4	
PIM-1@UiO-66	3590	250	310	5340	14.4	11.6	0.7	17.2	Ref[1]
PIM-1@Ti_5UiO-66	5280	660	1220	13540	8.0	4.3	0.4	11.1	Ref[1]
PIM-1@pDCX	9710	1130	1650	20550	8.6	5.9	0.5	12.5	Ref[2]
PIM-1@OH-pDCX	5230	300	380	8510	17.2	13.8	0.6	22.4	Ref[2]
PIM-1@ZIF-8	10650	1090	1440	17050	9.8	7.4	0.6	11.8	Ref[3]
PIM-1@Silica	7190	1800	NA	13400	4.0	NA	0.5	NA	Ref[3]
PIM-1@Silica-1	894	83	183	2530	10.8	4.9	0.4	13.8	Ref[3]
PIM-1@GCNN	3830	354	503	5785	10.8	7.6	0.7	11.5	Ref[3]
PIM-1*	1700	290	500	NA	5.8	3.4	NA	NA	Ref[4]
PIM-1/PAF-1*	5500	1200	2250	NA	4.5	2.4	NA	NA	Ref[4]
Original PIM-1	3731	309	431	6601	12.1	8.7	0.6	15.3	Ref[5]
PIM-UV 10min	3636	225	283	4560	16.2	12.8	0.8	16.1	Ref[5]
PIM-UV 20min	2818	73.6	62.1	1869	38.3	45.4	1.5	30.1	Ref[5]
PIM-UV 30min	2247	27.7	23.1	724	81.1	97.3	3.1	31.3	Ref[5]
PIM-UV 1h	1488	14.9	13.2	348	99.9	113	4.3	26.4	Ref[5]
PIM-UV 2h	553	4.9	4.7	118	112	118	4.7	25.1	Ref[5]
PIM-UV 4h	452	2.7	2.6	61.9	166	174	7.3	23.7	Ref[5]
P -79 µm	5343	623	991	12355	8.6	5.4	0.4	12.5	This work
P0.5	3741	259	323	6417	14.5	11.3	0.6	19.9	This work
P1.5	3528	104	97	3316	33.8	36.2	1.1	34.2	This work
P3.0-77 µm	2040	33	28	986	62.7	72.7	2.1	35.2	This work
P4.5	1028	9	8	158	109.4	127.1	6.5	19.5	This work
M	7066	638	902	12354	11.1	7.8	0.6	13.7	This work
M0.5	7257	326	340	8098	22.3	21.4	0.9	23.8	This work
M1.5	4676	94	78	2594	49.5	60.0	1.8	33.3	This work
M3.0	4769	68	53	2081	70.4	89.7	2.3	39.3	This work
M4.5	1535	18	16	374	86.2	93.5	4.1	23.4	This work
P3.0-47 µm	217	2	1.7	47	108	126	4.6	27.3	This work
P3.0-20 µm	106	0.85	0.75	22.3	125	142	4.8	30	This work
P3.0- ~ 1 µm	338	NA	48	388	NA	7.1	0.87	8.1	This work

Notice: P: PIM-1; M: PIM-1@PAF-1; 0.5, 1.5, 3.0, 4.5: UV 254 nm irradiation for as-cast membranes with 0.5, 1.5, 3.0 and 4.5 hours correspondingly.*: data estimated from ref. NA: Not Applicable

6. Mixed Gas Performance

Mixed gas permeabilities for CO_2 and CH_4 (50/50 mole ratio) at a partial pressure of 2 bar (total pressure 4 bar) and 35 °C were calculated by using the constant pressure method as illustrated in previous work.[6] A custom-built permeation cell, which contains a flow distributor, was used to prevent the concentration polarization at the upstream face of the membrane. The downstream pressure was atmospheric (0 psig), and a carrier gas (Helium) was used to sweep the permeate gas molecules away from the membrane surface to the gas chromatograph (GC). The gas composition stream was determined by an Agilent 6890 GC (Agilent Technologies, Santa Clara, CA, USA) with a thermal conductivity detector (TCD). All data from these measurements were collected when the steady-state transmembrane flux was reached, and the stage cut (i.e., the ratio of the feed flow rate to the permeation rate) was less than 0.1 %. Permeability was calculated using the following equation

$$P_{A=}\frac{x_{1A}S}{x_{He}^{P}A(p_2x_{2A}-P_1x_{1A})}L \qquad \text{Equation 2}$$

Where: P_A is the permeability coefficient of component A, S is the sweep gas (Helium) flow rate, $x_{1A}\ and\ x_{2A}$ are the mole fractions of component A in the permeate stream and feed streams respectively; x_{He}^{P} is the mole fraction of helium in the permeate stream, P_2 is the feed stream pressure, P_1 is the permeate stream pressure, A is the area of the membrane, and L is the membrane thickness.

Table S4 — **Mixed gas 50:50 CO_2:CH_4**

Sample	Permeability (Barrer)		Selectivity
	CO_2	CH_4	CO_2/CH_4
P	9927	1167	8.5
P3.0	5079	344	14.8
M	19020	3560	5.4
M3.0	6700	474	14.1

Notice: P:PIM-1; M:PIM-1@PAF-1; 3.0: UV irradiation 3.0 hour; experiment operated at 35 °C and 2 bar partial pressure, total pressure at 4 bar

Due to the different test methods, instruments, and conditions between single gas (constant volume, 25 °C) and mixed gas (constant pressure, 35 °C), the performance of single gas and mixed gas cannot be compared directly. However, this didn't take away the merits of PAF-1 and UV irradiation on PIM-1 membrane from mixed gas performance as similar synergistic effect observed compared to the single gas, that is, M3.0 exhibited a higher selectivity (66% up, 14 vs. 8.5) and retained permeability (6700 Barrer) compared to that of the pure PIM-1 membrane under mixed gas measurements.

7. Scanning Electron Microscopy (SEM)

A JEOL JSM-7001 Field Emission Scanning Electron Microscope (FESEM) with an accelerating voltage of 5 kV was used for imaging the cross-sectional surface of membrane samples. Cross-sectional surfaces, prepared by fracturing membranes in liquid nitrogen, were mounted using carbon tape, before sputter coating with iridium.

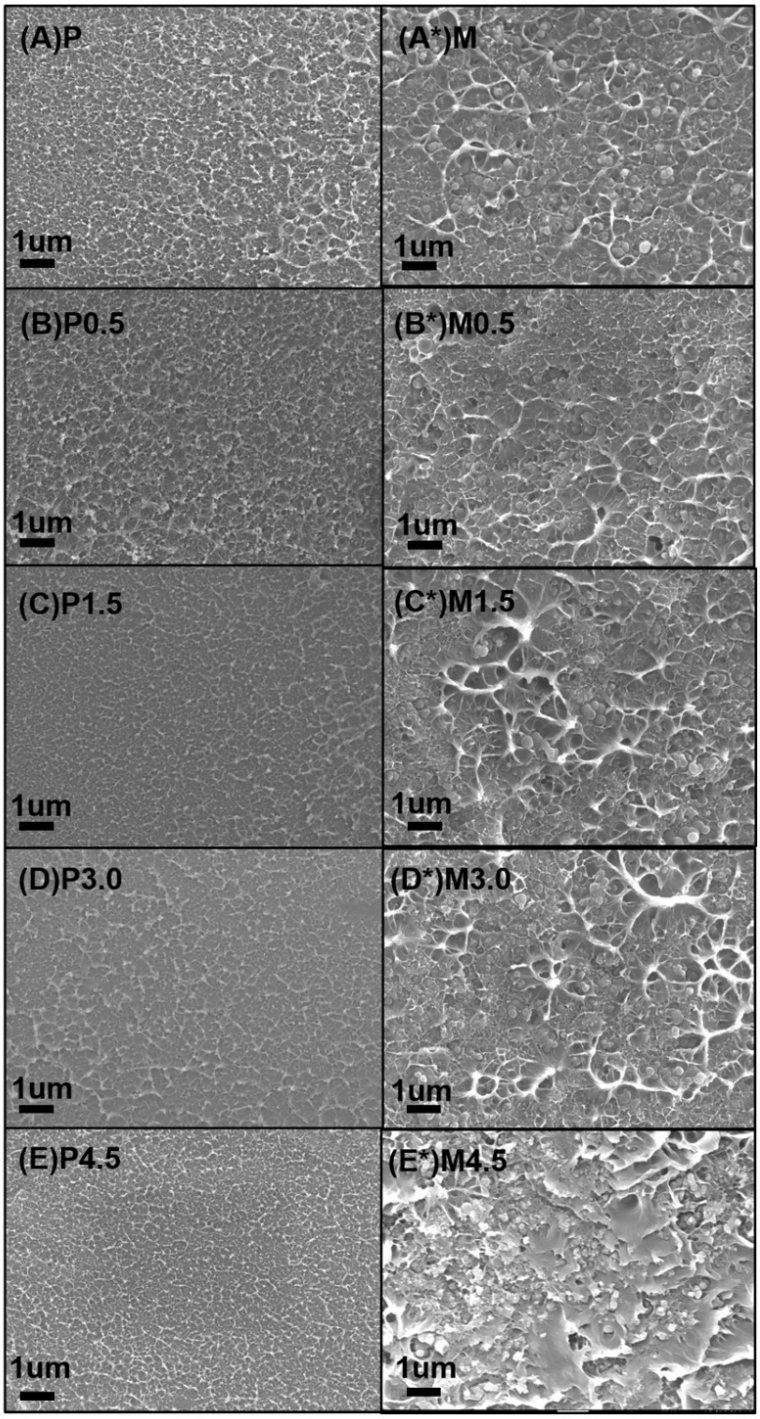

Figure S3. Cross-section SEM images for bulk membrane of P, P0.5, P1.5, P3.0, P4.5 and M, M0.5, M1.5, M3.0, M4.5. P: PIM-1; M: PIM-1@PAF-1; 0.5, 1.5, 3.0, 4.5 Stands for UV irradiation for 0.5, 1.5, 3.0 and 4.5 hours for pure PIM-1 and composite PIM-1@PAF-1 correspondingly.

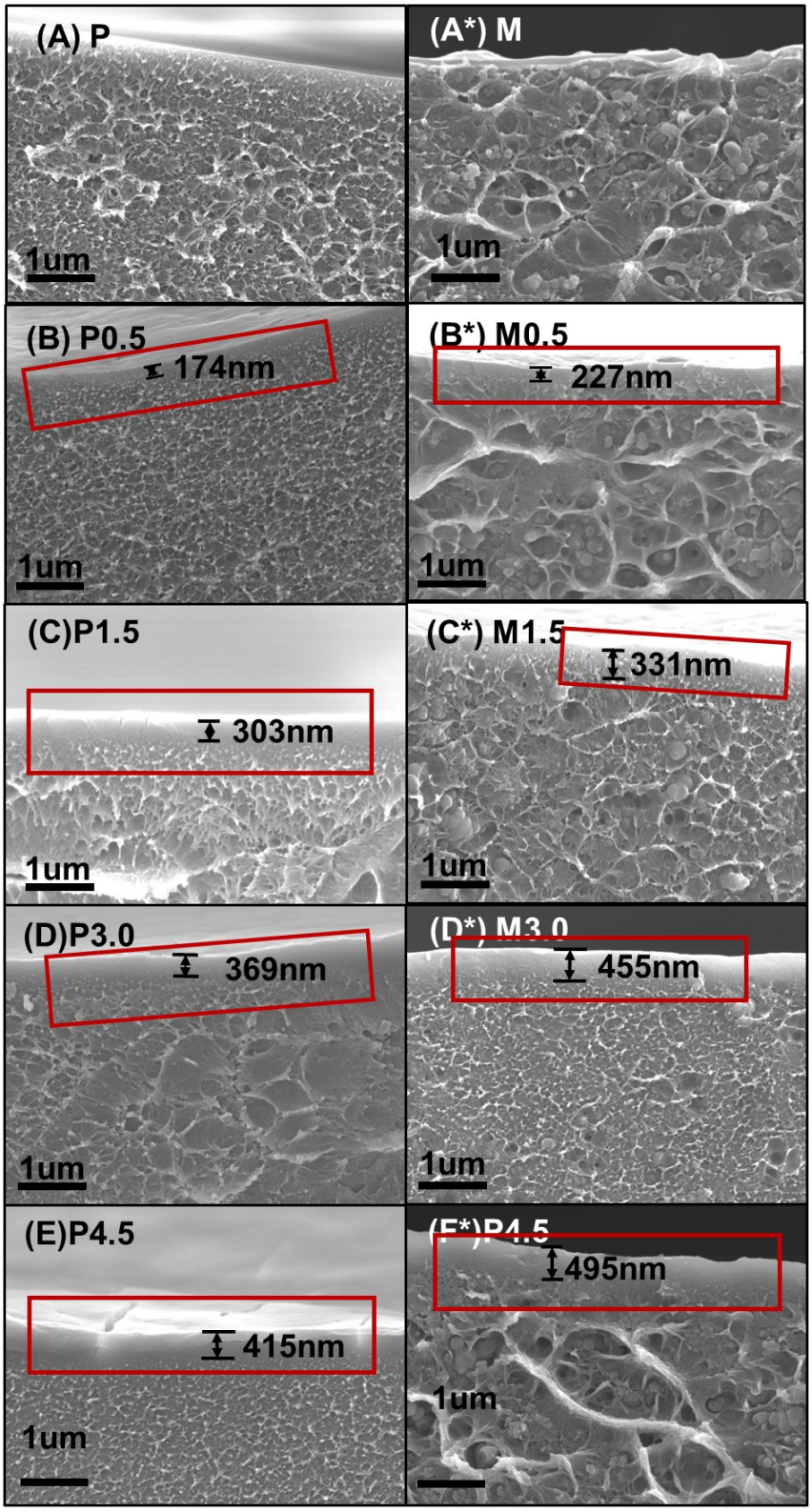

Figure S4. Cross-section SEM images for membrane near-surface area of P, P0.5, P1.5, P3.0, P4.5 and M, M0.5, M1.5, M3.0, M4.5. P: PIM-1; M: PIM-1@PAF-1; 0.5, 1.5, 3.0, 4.5 stands for UV irradiation for 0.5, 1.5, 3.0 and 4.5 hours for pure PIM-1 and composite PIM-1@PAF-1 correspondingly.

8. Positron Annihilation Lifetime Spectroscopy (PALS)

Average pore size and their relative abundance were obtained using Positron Annihilation Lifetime Spectroscopy. The membrane samples were cut and stacked into two 2 mm bundles and placed on either side of the sealed positron source in a Mylar envelope (^{22}NaCl, 1.8 MBq). The samples were placed in a vacuum cell (5 x 10^{-6} torr) between two EG&G Ortec fast-fast coincidence spectrometers. The timing resolution of the system was 240 ps, and a minimum of 5 files of 4.5 x 10^6 integrated counts were collected. The spectra were analysed using LT-v9 software [7] and fitted to 4 component lifetimes and a source correction (1.48 ns, 3.42%). The first lifetime (τ_1) was fixed to 0.125 ns and attributed to para-positronium (bound state of a positron and an electron with opposite spin) annihilation. The second component (τ_2) was due to free annihilation of the positron with free electrons within the sample. The longer lifetimes (τ_3, τ_4) were due to ortho-positronium annihilation of the positron in a bound state of an electron in the same spin state. These longer lifetimes are due to annihilation within the free volume of the membranes and indicate the presence of a bimodal porosity in the PIM-1 and the composite samples. The lifetimes were calculated using the Relative Tao-Eldrup relationship.[8-10] The pore size distribution was a visual representation adapted using the PAScual software.[11] The fractional free volume (FFV) calculation[12] was based on the equation below.

$$FFV_{PALS} = CV_{PALS}I_{PALS} \qquad \text{Equation S2}$$

where

$$V_{PALS} = \frac{4}{3}\pi R_{PALS}^{3} \qquad \text{Equation S3}$$

Here, C is the empirical constant, 0.0018 Å, V_{PALS} is the average volume of the pore elements calculated using the radius, R_{PALS} determined from the PALS lifetime and I_{PALS} is the associated Intensity. Separate pore size FFV (FFV 3 and FFV 4) and total FFV are listed in Table 1

Table S5 Positron Annihilation Lifetime Spectroscopy

	Pristine	MMM	$\frac{\Delta(MMM - \textbf{Pristine})}{Pristine}$	^{uv}MMM	$\frac{\Delta(uvMMM - \textbf{MMM})}{MMM}$	$\frac{\Delta(uvMMM - \textbf{Pristine})}{Pristine}$	^{uv}PIM-1	$\frac{\Delta(uvPIM1 - \textbf{Pristine})}{Pristine}$
Tau 3 (ns)	**2.881** (±0.209)	**3.484** (±0.160)		**3.144** (±0.230)			**2.949** (±0.35)	
Tau 4 (ns)	**8.589** (±0.173)	**10.350** (±0.204)		**9.265** (±0.181)			**8.437** (±0.292)	
I3(%)	**6.44** (±0.41)	**7.88 (±0.41)**	**+22.4%**	**6.73** (±0.37)	**-14.6%**	**+4.5%**	**6.61** (±0.76)	**+2.6%**
I4(%)	**15.88** (±0.54)	**15.16** (±0.44)	**-4.5%**	**16.10** (±0.51)	**+6.2%**	**+1.4%**	**15.29** (±0.93)	**-3.7%**
Diameter 3 (Å)	**7.10** (±0.029)	**7.89** (±0.019)	**+11.1%**	**7.42** (±0.030)	**-6.0%**	**+4.5%**	**7.20** (±0.048)	**+1.4%**
Diameter 4 (Å)	**12.24** (±0.011)	**13.30** (±0.012)	**+8.7%**	**12.67** (±0.011)	**-4.7%**	**+3.5%**	**12.15** (±0.019)	**-0.7%**

Note: Pristine: PIM-1; MMM: PIM-1@PAF-1; ^{uv}MMM: UV treated PIM-1@PAF-1; ^{uv}PIM-1: UV treated PIM-1; ±: Deviation

9. FT-IR Spectra of Membrane and Nanoparticle Samples

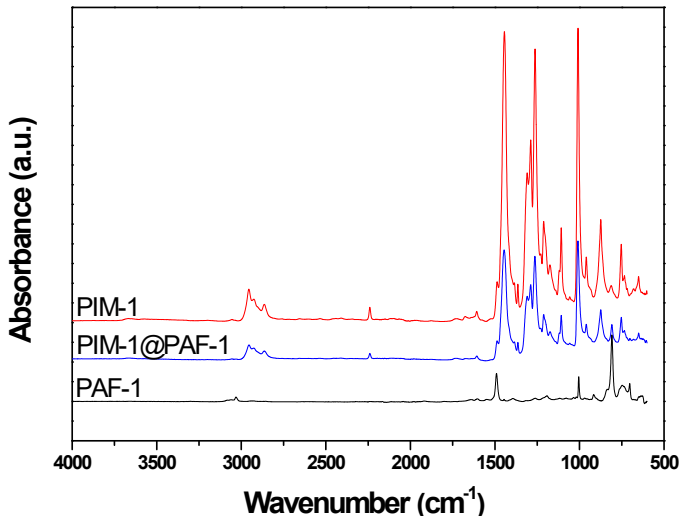

Figure S5a. FT-IR spectra of PIM-1, PIM-1@PAF-1, and PAF-1 samples

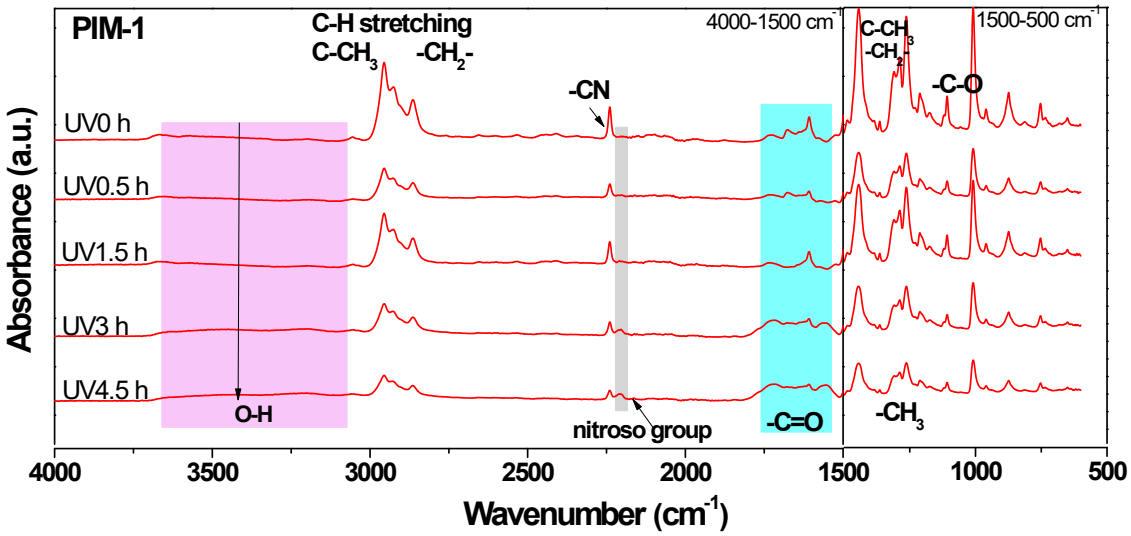

Figure S5b: FT-IR spectra of PIM-1 and UV treated PIM-1 with 0.5, 1.5, 3, and 4.5 h, respectively.

10. X-ray Photoelectron Spectroscopy (XPS)

X-ray photoelectron spectroscopy (XPS) analysis was performed using an AXIS Nova spectrometer (Kratos Analytical Inc., Manchester, UK) with a monochromated Al K_α source at a power of 180 W (15 kV × 12 mA), a hemispherical analyser operating in the fixed analyser transmission mode, and the standard aperture (analysis area: 0.3 mm × 0.7 mm). The total pressure in the main vacuum chamber during analysis was typically between 10^{-9} and 10^{-8} mbar. Survey spectra were acquired at a pass energy of 160 eV and step size of 0.5 eV. To obtain more detailed information about chemical structure, oxidation states, etc., high resolution spectra were recorded from individual peaks at 20 eV pass energy and step size of 0.1 eV, typically yielding a FWHM for the ester peak in PET of less than 0.85 eV during performance tests.

Each specimen was analysed at an emission angle of 0° as measured from the surface normal. Assuming typical values for the electron attenuation length of relevant photoelectrons, the XPS analysis depth (from which 95 % of the detected signal originates) ranges between 5 and 10 nm for a flat surface.

Depth profiling experiments were conducted using an Ar Gas Cluster Ion Source (GCIS; Kratos Analytical Inc. Minibeam 6) operated at a cluster size of Ar_{1000}^+ with an impact energy of 10 keV, equating to a partition energy of 10 eV per atom. For the ion beam, a raster size of 1.4 x 1.4 mm^2 was employed. A stable beam current was confirmed prior to depth profiling by measuring the sample current on the earthed sample platen. Samples were etched five times for the following amount of time: 10 s, 20 s, 30 s, 90 s and 120 s.

Data processing was performed using CasaXPS processing software version 2.3.15 (Casa Software Ltd., Teignmouth, UK). All elements present were identified from survey spectra. The atomic concentrations of the detected elements were calculated using integral peak intensities and the sensitivity factors supplied by the manufacturer. A three-parameter Tougaard background[13] was employed using the default parameters for polymers (Cross Section: 551, 436, 3). A generalised Voigt lineshape was employed for synthetic components used in peak fitting, represented by LA() and LF() in CasaXPS, specifically LF(1,1,10,300), for all components with the exception of N1 – LF(1,1,15,200). Binding energies were referenced to the C 1s peak at 284.8 eV (aromatic hydrocarbon).

The accuracy associated with quantitative XPS is ca. 10% - 15%.

Precision (ie. reproducibility) depends on the signal/noise ratio but is usually much better than 5%. The latter is relevant when comparing similar samples.

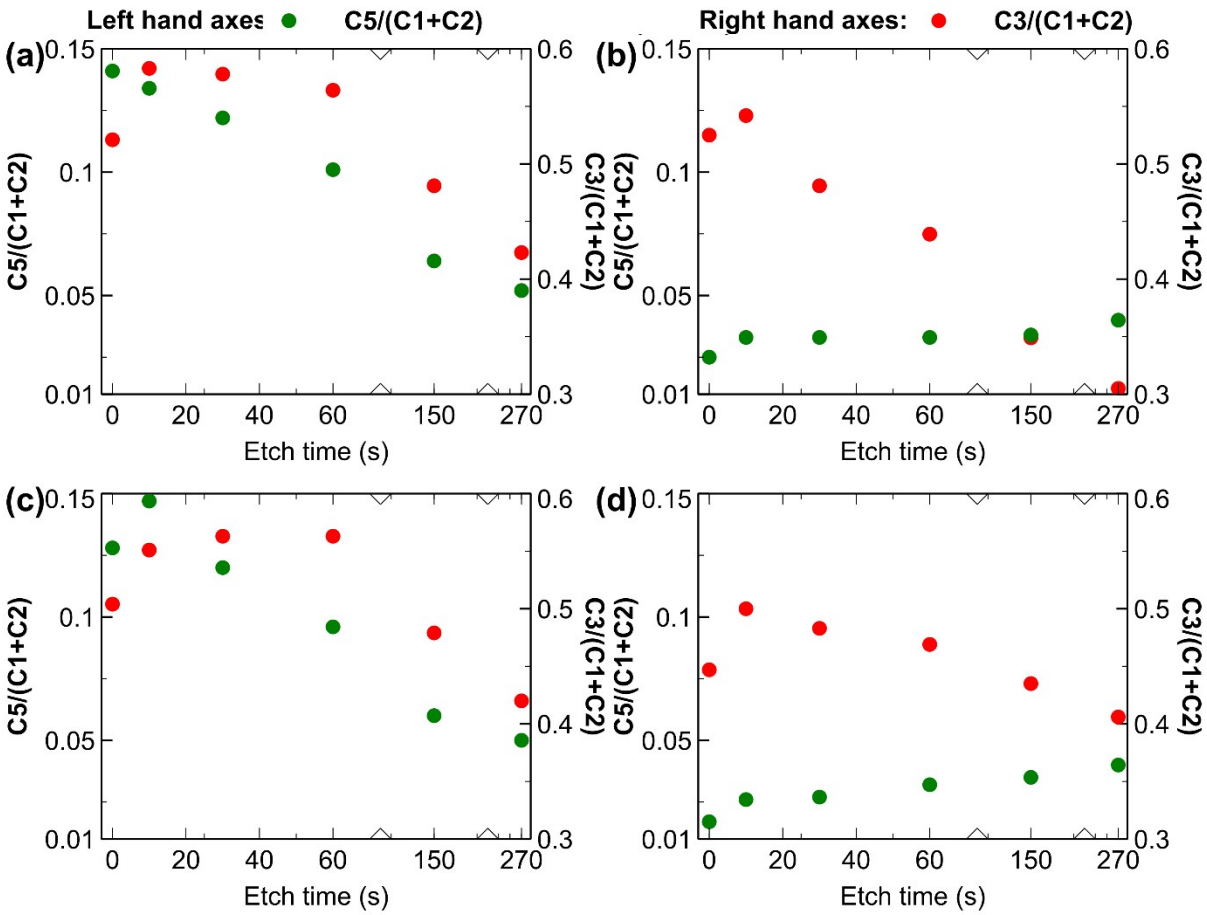

Figure S6: Relative fraction of C (%), specifically components C5 (O-C=O) and C3 (C-O), normalised by hydrocarbon contribution (C1+C2) derived from fitting of high-resolution C 1s spectra as demonstrated in Figure S7 (**a)** M4.5 (PIM-1@PAF-1 with 4.5 hour UV irradiation)**; (b)** M (PIM-1@PAF-1)**; (c)** P4.5 (PIM-1 with 4.5 hours UV irradiation)**; (d)** P (PIM-1)**.** For UV treated samples, we observe more C5 and C3, consistent with elemental quantification.

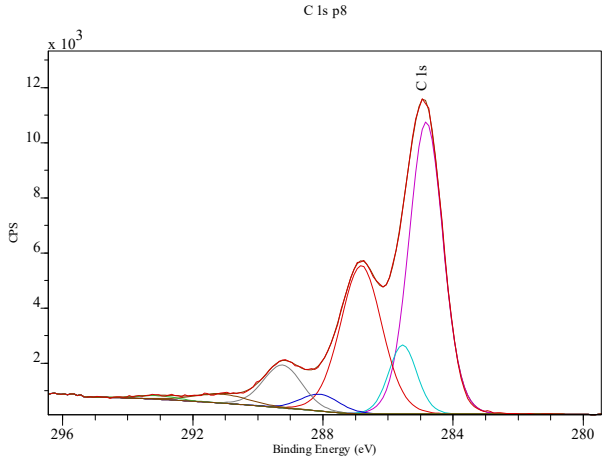

Figure S7: Selected representative, high resolution C 1s of UV-treated M4.5 (PIM-1@PAF-1 with 4.5 hours UV irradiation) membrane sample. A 7 component system was employed with the following assignments[14]: C1+C2 = C-C, C-H; C3 = C-O, C≡N; C4 = O-C-O, C=O, N-C=O; C5 = O-C=O; C6+C7 = shake-up.

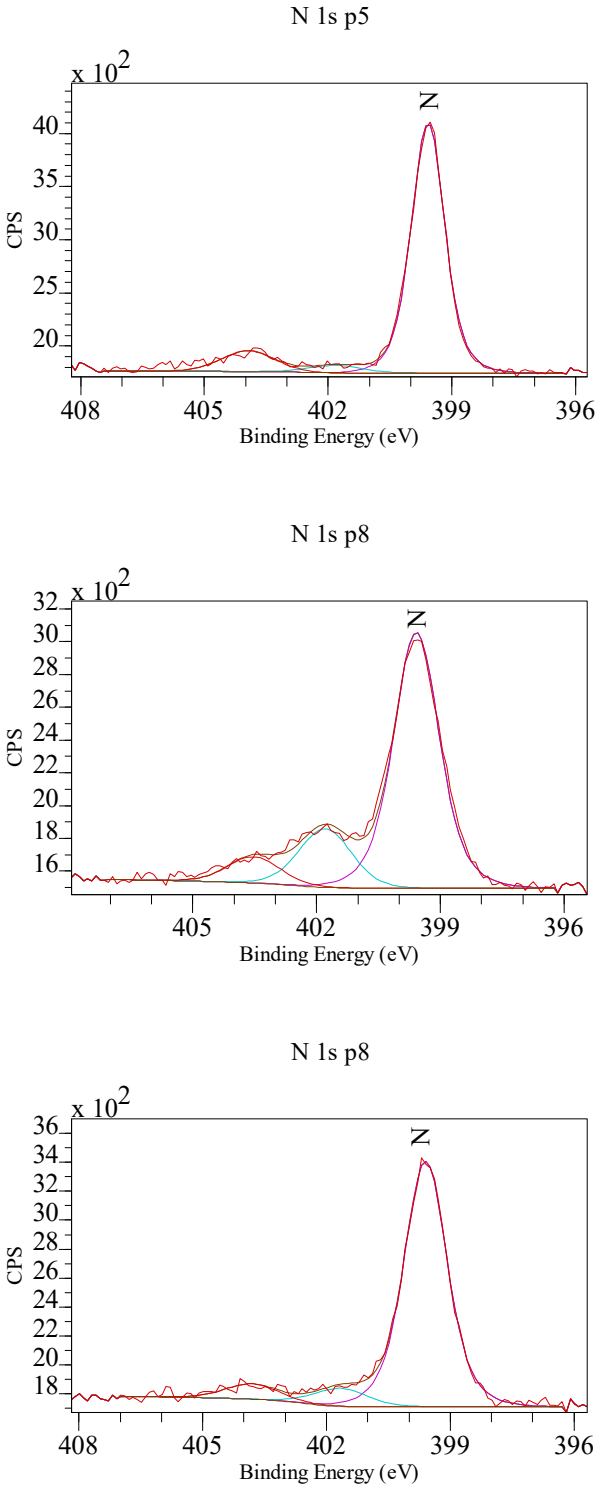

Figure S8: Selected, representative, high resolution N 1s of the M (top panel, PIM-1@PAF-1) and M4.5 (middle panel, PIM-1@PAF-1 with 4.5 hours UV irradiation) membrane samples at etch time 0 s, and M4.5 (bottom panel) after final etch. A 3 component system was employed with the following assignments[14-16]: N1 = N≡C; N2 = N+, NO; N3 = undefined.

11. Gel Fraction Test

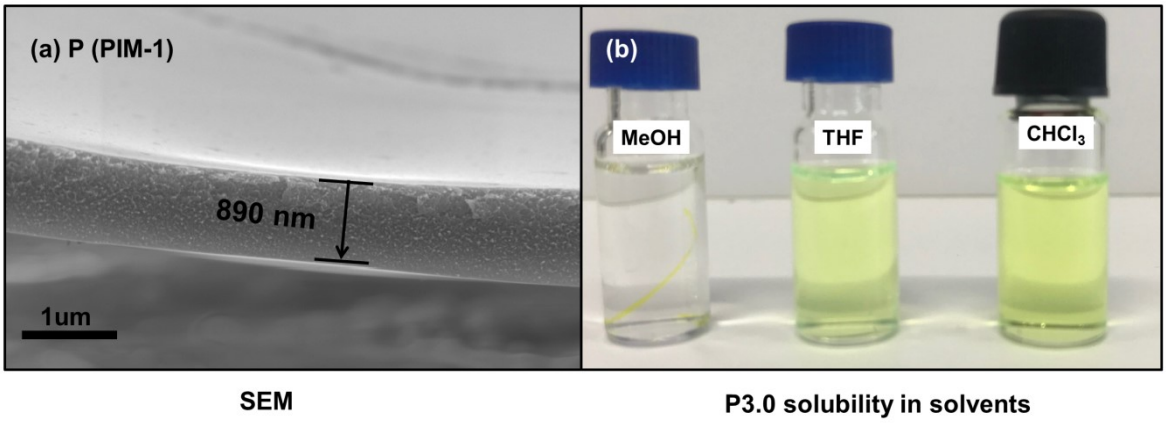

Figure S9. (a) Cross-section of thin membrane fabricated from the spin-coating method**. (b)** 3 h of UV treated PIM-1 solubility in different solvents.

12. Membrane Long -term Study

The aging study of the polymer films involved storing the samples under ambient conditions after initial membrane performance measurements for as-cast samples. To reflect membrane intrinsic physical aging properties, the long-term study compared the performance of membranes aged 15 days and 60 days. The typical fast physical aging behaviour during the first two weeks is due to the rapidly collapsed excess free volume resulting from methanol soaking, as described in the work of Piannu *et al.*[17] Permeation measurements were carried out on these aged membranes after evacuating overnight to remove any adsorbed air and any other potential impurities from storage. For each test, single gas measurements were recorded sequentially using H_2, N_2, CH_4, and CO_2 at 2 bar feed pressure, in duplicate (deviation with ± 10%) at 25 ± 1 °C. Before changing gases for permeation testing, the membrane and permeation system was evacuated under a low vacuum for at least 2 hours to completely remove prior gas and ensure the measurement accuracy.

As seen in Figure S10, either PAF-1 incorporated PIM-1, or UV treated PIM-1, or samples that combined these two functions, demonstrated a slower physical aging rate than the native PIM-1 membrane, which was consistent with previous studies. [18] [19, 20]

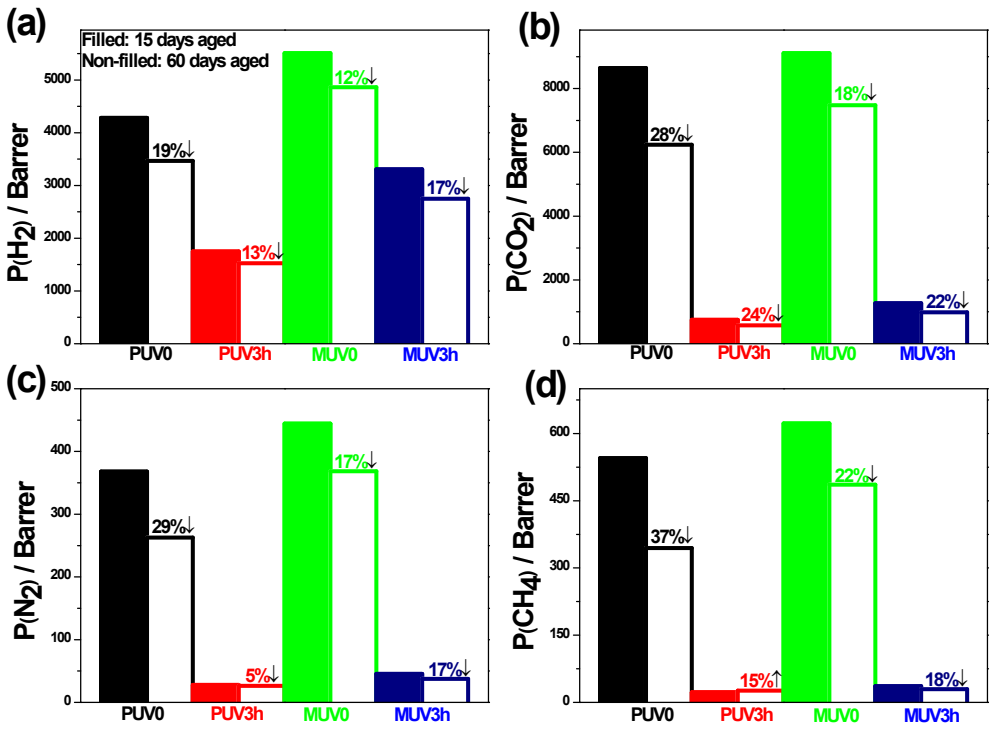

Figure S10. Long-term stability test over 60 days for **(a)** H_2, **(b)** CO_2, **(c)** N_2, and **(d)** CH_4 for membranes of PUV0, PUV3h, MUV0, and MUV3h.

13. Thin Membrane Gas Permeation Summary

The thin membrane with the highest selectivity was chosen to compare its performance with thick membranes in **Figure 9.**

Table S6 **UV 254 nm Irradiation effect**

		0.0h	0.5h	1.0h	2.0h	3.0h	
PIM-1/ PDMS/ PAN	H_2	515	537	512	444	414	**Permeance (GPU)**
	CH_4	225	201	172	158	161	
	CO_2	988	834	584	315	267	
	H_2/CH_4	2.3	2.7	3.0	2.8	2.6	**Selectivity**
	CO_2/CH_4	4.4	4.2	3.4	2.0	1.7	
PIM-1/ PAF-1/ PDMS/ PAN	H_2	626	544	500	412	368	**Permeance (GPU)**
	CH_4	419	369	331	295	294	
	CO_2	1699	1478	1242	1040	981	
	H_2/CH_4	1.5	1.5	1.4	1.4	1.3	**Selectivity**
	CO_2/CH_4	4.1	4.0	3.5	3.5	3.3	
PIM-1/ PAN	H_2	565	439	338	162	NA	**Permeance (GPU)**
	CH_4	129	71	48	37	NA	
	CO_2	1240	782	388.3	86	NA	
	H_2/CH_4	4.4	6.2	7.1	4.4	NA	**Selectivity**
	CO_2/CH_4	9.7	10.9	8.1	2.3	NA	

Notice: operation conditions: Dead cell, single gas, 3 atm, 35°C. composite membrane with 10wt% PAF-1 loading

14. References

1. S. J. D. Smith, B. P. Ladewig, A. J. Hill, C. H. Lau and M. R. Hill, *Scientific Reports*, 2015, **5**, 7823.
2. R. Hou, S. J. D. Smith, C. D. Wood, R. J. Mulder, C. H. Lau, H. Wang and M. R. Hill, *ACS Applied Materials & Interfaces*, 2019, **11**, 6502-6511.
3. R. Castro-Muñoz, V. Fila and C. Dung, *Chemical Engineering Communications*, 2017, **204**, 295-309.
4. C. H. Lau, K. Konstas, A. W. Thornton, A. C. Y. Liu, S. Mudie, D. F. Kennedy, S. C. Howard, A. J. Hill and M. R. Hill, *Angewandte Chemie International Edition*, 2015, **54**, 2669-2673.
5. F. Y. Li, Y. Xiao, Y. K. Ong and T.-S. Chung, *Advanced Energy Materials*, 2012, **2**, 1456-1466.
6. C. H. Lau, K. Konstas, C. M. Doherty, S. J. D. Smith, R. Hou, H. Wang, M. Carta, H. Yoon, J. Park, B. D. Freeman, R. Malpass-Evans, E. Lasseuguette, M.-C. Ferrari, N. B. McKeown and M. R. Hill, *Nanoscale*, 2020, **12**, 17405-17410.
7. J. Kansy, *Nuclear Instruments and Methods in Physics Research Section A: Accelerators, Spectrometers, Detectors and Associated Equipment*, 1996, **374**, 235-244.
8. S. Tao, *The Journal of Chemical Physics*, 1972, **56**, 5499-5510.
9. M. Eldrup, D. Lightbody and J. N. Sherwood, *Chemical Physics*, 1981, **63**, 51-58.
10. T. Dull, W. Frieze, D. Gidley, J. Sun and A. Yee, *The Journal of Physical Chemistry B*, 2001, **105**, 4657-4662.
11. C. Pascual-Izarra, A. W. Dong, S. J. Pas, A. J. Hill, B. J. Boyd and C. J. Drummond, *Nuclear Instruments and Methods in Physics Research Section A: Accelerators, Spectrometers, Detectors and Associated Equipment*, 2009, **603**, 456-466.
12. Yuri Yampolskii and i. Shantarovich, *John Wiley & Sons, Ltd. ISBN: 0-470-85345-X*, 2006.
13. S. Tougaard, *Surface and Interface Analysis*, 1997, **25**, 137-154.
14. G. A. George, *Polymer International*, 1994, **33**, 439-440.
15. J. R. Pels, F. Kapteijn, J. A. Moulijn, Q. Zhu and K. M. Thomas, *Carbon*, 1995, **33**, 1641-1653.
16. C. D. Batich and D. S. Donald, *Journal of the American Chemical Society*, 1984, **106**, 2758-2761.
17. B. S. Ghanem, R. Swaidan, X. Ma, E. Litwiller and I. Pinnau, *Advanced Materials*, 2014, **26**, 6696-6700.
18. F. Y. Li and T.-S. Chung, *International Journal of Hydrogen Energy*, 2013, **38**, 9786-9793.
19. C. H. Lau, P. T. Nguyen, M. R. Hill, A. W. Thornton, K. Konstas, C. M. Doherty, R. J. Mulder, L. Bourgeois, A. C. Y. Liu, D. J. Sprouster, J. P. Sullivan, T. J. Bastow, A. J. Hill, D. L. Gin and R. D. Noble, *Angewandte Chemie International Edition*, 2014, **53**, 5322-5326.
20. C. H. Lau, K. Konstas, A. Thornton, A. Liu, S. Mudie, D. Kennedy, S. Howard, A. Hill and M. Hill, *Angewandte Chemie International Edition in English* 2015, **54**, 2669-2673.